Multiproxy evidence of the Neoglacial expansion of Atlantic Water to eastern Svalbard: Does ancient environmental DNA complement sedimentary and microfossil records?

Joanna Pawłowska[1*], Magdalena Łącka[1], Małgorzata Kucharska[1], Jan Pawlowski[2], Marek Zajączkowski[1]

[1]Institute of Oceanology Polish Academy of Sciences, Sopot, 81-712, Poland

[2]Department of Genetics and Evolution, University of Geneva, Geneva, CH 1211, Switzerland

Correspondence to: Joanna Pawłowska (pawlowska@iopan.pl)

Abstract. The main goal of this study was to reconstruct the paleoceanographic development of Storfjorden during the Neoglacial (~ 4 cal ka BP). Storfjorden is one of the most important "brine factory" in the European Arctic, responsible for deep water production. Moreover, it is a climate-sensitive area, influenced by two contrasting water masses: warm and saline Atlantic Water (AW) and colder and fresher Arctic Water (ArW). Herein, a multiproxy approach was applied to provide evidence for interactions between the inflow of AW and sea-ice coverage, which are the major drivers of environmental changes in Storfjorden. The sedimentary and microfossil records indicate that a major reorganization of oceanographic conditions in Storfjorden occurred at ~ 2.7 cal ka BP. A general cooling and the less pronounced presence of AW in Storfjorden during the early phase of the Neoglacial are prerequisite conditions for the formation of an extensive sea-ice cover. The period after ~ 2.7 cal ka BP was characterized by alternating short-term cooling and warming intervals. Warming was associated with pulsed inflows of AW and sea-ice melting that stimulated phytoplankton blooms and organic matter supply to the bottom. The cold phases were characterized by heavy and densely packed sea ice resulting in a decrease in productivity. The ancient environmental DNA (aDNA) records of foraminifera and diatoms reveal the timing of the major pulses of AW (~2.3 and ~1.7 cal ka BP) and the variation in sea-ice cover. The AW inflow was marked by an increase in the percentage of DNA sequences of monothalamous foraminifera associated with the presence of fresh phytodetritus, while cold and less productive intervals were marked by an increased proportion of monothalamous taxa known

only from environmental sequencing. The diatom aDNA record indicates that primary production was continuous during the Neoglacial regardless of sea-ice conditions. However, the colder periods were characterized by the presence of diatom taxa associated with sea ice, whereas the present-day diatom assemblage is dominated by open-water taxa.

1. Introduction

The flow of Atlantic Water (AW) is one of the major heat contributors to the Arctic Ocean (Polyakov et al., 2017). Recent oceanographic data indicate warming due to an increase in AW in the Arctic Ocean (Rudels et al., 2015, Polyakov et al., 2017). AW has been present along the western margin of Svalbard during at least the last 12,000 years (e.g., Werner et al., 2011; Rasmussen et al., 2014). One of the major intrusions of AW occurred during the early Holocene (10.8 – 6.8 cal ka BP). A distinct cooling and freshening of the bottom water masses occurred during the mid-late Holocene (6.8–1 cal ka BP) and was accompanied by glacier readvances in Svalbard leading to present-day conditions (Ślubowska-Woldengen et al., 2007; Telesiński et al., 2018). The paleoceanographic conditions in the Svalbard margins correlate closely to the sea surface temperature (SST) variations in the Nordic Seas and confirm that the Svalbard area is highly sensitive to fluctuations in the inflow of AW (Ślubowska-Woldengen et al., 2007). Conversely, until the 1990s eastern Svalbard was recognized as an area exclusively influenced by the East Spitsbergen Current (ESC), which carries cold and less saline Arctic Water (ArW) from the Barents Sea (e.g., Quadfasel et al., 1988; Piechura et al., 1996). Recent studies have revealed that the oceanography of the area is much more complicated (e.g. Skogseth et al., 2007; Geyer et al., 2010). Oceanographic data obtained from conductivity–temperature sensors attached to *Delphinapterus leucas* show a substantial contribution of AW to Storfjorden (east Spitsbergen; Lydersen et al., 2002). Recently, a suggestion by Hansen et al. (2011) that AW was present in Storfjorden during the early Holocene warming (11 – 6.8 cal ka BP) was confirmed by Łącka et al. (2015). However, the limited amount of data available for eastern Svalbard often makes paleoceanographic reconstructions of the area speculative.

The latter part of the Holocene, the so-called Neoglacial cooling (~ 4 cal ka BP), in the European Arctic is correlated with a decline in the summer insolation at northern latitudes (Berger, 1978) and a decline in summer SST (Andersen et al., 2004; Risebrobakken et al., 2010; Rasmussen et al., 2014a). The cooling of the surface waters and the limited AW inflow to the Nordic Seas led to the formation of an extended sea-ice cover (Müller et al., 2012). In addition, the southwestern and eastern shelf of Spitsbergen experienced a strengthening of the

East Spitsbergen Current leading to an intensification of ArW inflow and the formation of an extensive sea-ice cover (Sarnthein et al., 2003). Therefore, the Neoglacial has usually considered a constantly cold period, with a culmination of cooling during the Little Ice Age. However, the records from Storfjorden and the Barents Sea suggest that the Neoglacial was a period of variable oceanographic conditions with strong temperature and salinity gradients (Calvo et al., 2002; Martrat et al., 2003; Sarnthein et al., 2003; Łącka et al., 2015). There is also evidence of episodic intensifications of the warm AW inflow to western Svalbard at that time (e.g. Risebrobakken et al. 2010; Rasmussen et al., 2012).

According to Nilsen et al. (2008), the critical parameter controlling the fjord–shelf exchange is the density difference between the fjord water masses and the AW. The local winter ice production and formation of brine-enriched waters determines the density of local water masses, which is a key factor that enables AW to penetrate into fjords during the spring and summer. Moreover, the production of brine-enriched waters and associated deep-water overflow is a key contributor to large-scale ocean circulation (Killworth, 1983). In this respect, Storfjorden is especially important because it is one of the few areas where brine-enriched waters have been frequently observed (Haarpainter et al., 2001). In the last decades, reduced brine formation occurred during periods with the most intensive AW advection to Storfjorden and reduced sea-ice formation in the Barents Sea, while intense brine formation was re-established during periods of recurrent cooling (Årthun et al., 2011).

The aim of the presented study is to reconstruct the paleoceanographic development of Storfjorden during the Neoglacial with multicentennial resolution. We assumed that the periodic intensification of the AW inflow to the West Spitsbergen shelf during the Neoglacial resulted in the appearance of AW also in eastern Spitsbergen, similar to the early Holocene (e.g., Łącka et al., 2015), affecting the density and extent of sea-ice cover in the area. A multiproxy approach comprising composed of sedimentary, microfossil and molecular records was applied to provide evidence for interactions between the inflow of AW and sea-ice coverage in Storfjorden. The ancient environmental DNA (aDNA) analysis targeted diatoms and nonfossilized monothalamous foraminifera, groups that are hardly preserved in fossil records from the Spitsbergen fjords (Pawłowska et al., 2014, Łącka M., *pers. commun.*) Recent studies have demonstrated that analyses of genetic material obtained directly from environmental samples (so called environmental DNA) are an efficient method for biodiversity surveys across time and space (Thomsen and Willerslev, 2015). Our previous studies of foraminiferal aDNA revealed the extraordinary richness of the foraminiferal community, primarily due to the detection of soft-walled monothalamous taxa (Pawłowska et

al., 2014). Furthermore, aDNA has been proven to be an effective tool in paleoceanographic reconstructions (e.g. Boere et al., 2009; Pawłowska et al., 2016). The molecular data correlated well with environmental changes and even revealed small changes that were not clearly indicated by other proxy records (Pawłowska et al., 2016). The combination of aDNA studies with the analysis of microfossils and sedimentary proxies provides a powerful means to reconstruct past environments more comprehensively.

2. Study area

Storfjorden is located in southeastern Svalbard between the islands of Spitsbergen, Edgeøya and Barentsøya. Storfjorden is ~190 m long and its main basin is ~190 m deep. Two narrow and shallow passages Heleysundet and Freemansundet connect northern Storfjorden to the Barents Sea. To the south, a 120-m-deep sill separates the main basin from the Storfjordrenna Trough. Storfjordrenna is 245 m long, with a depth varying from 150 m to 420 m.

The water masses in Storfjorden are composed primarily of exogenous Atlantic and Arctic waters and mixed waters that have formed locally. Warm AW is transported by the West Spitsbergen Current branches off near Storfjordrenna and enters the southern part of the fjord. Arctic water (ArW) from the Arctic Ocean and the Barents Sea enters Storfjorden via two passages to the northeast and continues along the inner shelf of Svalbard as a coastal currents. AW is characterized by temperatures > 3 °C and salinity > 34.95, while the temperature and salinity of ArW are < 0 °C and 34.3-34.8, respectively. The presence of locally formed water masses is a result of the interactions between AW, ArW and melt water. Skogseth et al. (2005) listed six local water masses: melt water (MW), polar front water (PW), East Spitsbergen water (ESW), brine-enriched shelf water (BSW), Storfjorden surface water (SSW), and modified Atlantic water (MAW). BSW is formed due to the release of large amounts of brines during polynya events and the intensive formation of sea ice (Haarpainter et al., 2001; Skogseth et al., 2004, 2005) and is characterized by salinities exceeding 34.8 and temperatures below -1.5 °C (Skogseth et al., 2005).

The sedimentary environment in Storfjorden classified as a low-energy, high-accumulation environment, characteristic of inner fjords. The area is sheltered from along-shelf bottom currents and is affected by high terrigenous inputs; therefore deposition prevails over sediment removal by bottom currents (Winklemann and Knies, 2005). The primary productivity is high and strongly depends on the sea ice formation and the duration of the marginal ice zone (Winkelman and Knies, 2005).

3. Materials and methods

3.1 Sampling

The 55-cm-long sediment core ST_1.5 was taken with a gravity corer in Storfjorden during cruise of the R/V *Oceania* in August 2014. The sampling station was located at 76° 53,181' N and 19° 27,559' E at a depth of 153 m (Fig. 1). The core was stored at 4°C and shipped to the Institute of Oceanology PAS for further analyses.

In the laboratory, the core was extruded and cut into 1-cm slices. During cutting, sterile subsamples for ancient DNA (aDNA) analyses were taken at 5 cm intervals. To avoid extraneous and/or cross-contamination the thin layers of sediment that were in contact with under- or overlying sediments were removed using a sterile spatula. Samples for aDNA analyses were kept frozen in -20°C.

3.2 Sediment dating

The chronology of the sediment layers is based on high-precision accelerator mass spectrometry (AMS) ^{14}C dating performed on five bivalve shells from the sediment layers at 2.5, 5.5, 14.5, 43.5, 52.5 cm and on foraminifera *Nonionellina labradorica* from sediment depth of 46.5 cm. The bivalve shells were identified to the highest possible taxonomic level and processed on the 1.5 SDH-Pelletron Model "Compact Carbon AMS" in the Poznań Radiocarbon Laboratory, Poznań, Poland. Dating of foraminiferal tests were performed at the National Ocean Sciences AMS (NOSAMS) laboratory in the Woods Hole Oceanographic Institution, Woods Hole, MA, USA. The dates were converted into calibrated ages using the calibration program CALIB Rev. 7.1.0 Beta (Stuiver and Reimer, 1993) and the Marine13 calibration dataset (Reimer et al., 2013). A difference (ΔR) in the reservoir age correction of 105 ± 24 was applied (Mangerud et al., 2006). The calibrated results are reported in units of thousand calibrated years BP (cal ka BP), see Table 1.

3.3 Sediment grain size

Samples for the grain size analyses were freeze-dried and milled. Measurements were performed using a Mastersizer 2000 particle laser analyzer coupled to a Hydro MU device (Malvern, UK). Samples were treated with ultrasound to avoid aggregation. Raw data were analyzed using GRADISTAT v.8.0 software (Blott and Pye, 2001). The mean 0-63-μm grain size [φ] was calculated via the logarithmic method of moments. The sediment fraction >500 μm was used for an ice rafted debris (IRD) analysis. Grains were counted under a

stereomicroscope and the amount of IRD is reported as the number of grains per gram of dry sediment [grains g^{-1}] and flux [grains cm^{-2} y^{-1}].

3.4 Fossil foraminifera

Prior to fossil foraminifera analysis, samples were wet sieved through a mesh with 500-µm and 100-µm openings and dried at 60°C. Samples with large quantities of tests were divided using a microsplitter. At least 300 specimens of benthic foraminifera were isolated from each sample and collected on micropaleontological slides. Benthic foraminifera specimens were counted and identified to the lowest possible taxonomic level. The quantity of foraminifera is presented as the number of individuals per gram of dry sediment [ind. g^{-1}] and flux [ind. cm^{-2} y^{-1}]. Foraminifera species were grouped according to their ecological tolerances. Four groups of indicators were distinguished: AW/frontal zone indicators, ArW indicators, bottom current indicators and glaciomarine species (Majewski et al., 2009). Morphologically similar species *Islandiella norcrossi* and *Islandiella helenae* are reported as *Islandiella* spp.

3.5 Stable isotopes analysis

Carbon and oxygen stable isotope analyses were performed on *Cibicidoides lobatulus* tests selected from 27 sediment layers. From 10 to 12 specimens were collected from each sample and subjected to ultrasonic cleaning. The measurements were performed on a Finningan MAT 253 mass spectrometer coupled to a Kiel IV carbonate preparation device at the University of Florida. The resulting values are expressed in standard δ notation relative to Vienna Pee Dee Belemnite (VPDB).

3.6 Ancient DNA analysis

Total DNA was extracted from approximately 10 g sediment using a Power Max Soil DNA extraction kit (MoBio). The foraminiferal SSU rDNA fragment containing the 37f hypervariable region was PCR amplified using primers tagged with unique sequences of five nucleotides appended to their 5' ends (denoted by Xs), namely the foraminifera-specific forward primer s14F1 (5'-XXXXXCGGACACACTGAGGATTGACAG-3') and the reverse primer s15 (5'-XXXXXCCTATCACATAATCATGAAAG-3'). The diatom DNA fragment located in the V4 region was amplified with the forward DIV4for (5'-XXXXXXXXGCGGTAATTCCAGCTCCAATAG-3') and reverse DIV4rev3 (5′-

XXXXXXXXCTCTGACAATGGAATACGAATA-3') primers tagged with a unique combination of eight nucleotides (denoted by Xs) attached at each primer's 5'-extremity. The amplicons were purified using the High Pure PCR Cleanup Micro Kit (Roche) and quantified using a Qubit 2.0 fluorometer. Samples were pooled in equimolar quantities and the sequence library was prepared using a TruSeq library-preparation kit (Illumina). Samples were then loaded into a MiSeq instrument for a paired-end run of 2*150 cycles (foraminifera) and 2*250 cycles (diatoms). The processing of the HTS sequence data was performed according to procedures described by Lejzerowicz et al. (2013) and Pawłowska et al. (2014). The post-sequencing data processing was performed with the use of SLIM web app (Dufresne et al., 2019) and included demultiplexing the libraries, joining the paired-end reads, chimera removal, Operational Taxonomic Units (OTUs) clustering, and taxonomic assignment. Sequences were clustered into OTUs using Swarm module (Mahe et al. 2014) and each OUT was assigned to the highest possible taxonomic level using vsearch (Rognes et al., 2016) against a local database and then reassigned using BLAST (Altschul et al., 1990). The results are presented in OTU-to-sample tables and transformed in terms of the number of sequences, number of OTUs and the percentage (%) of sequences.

4. Results

4.1 Sediment age and type

All dates were in the chronological order and the uppermost layer contained modern, post-bomb carbon indicating a post-1960 age (Table 1). Samples from depths of 2.5 cm and 5.5 cm were not calibrated because they revealed ages that were invalid for the selected calibration curve. The age model was therefore based on the three remaining dates using a linear interpolation. The age of the bottom of the core was estimated to be approximately 7.9 cal ka BP (Fig. 3). However, the extremely low time resolution between 7.9 cal ka BP and 4 cal ka BP precluded making any general conclusion about that interval. Therefore, the manuscript focuses only on the last 4 cal ka BP (the Neoglacial).

The sediment accumulation rate (SAR) prior to ~ 2.7 cal ka BP was 0.002 cm y^{-1}. The approximately 10-fold increase in SAR is noted at ~ 2.7 cal ka BP, when it increased to 0.023 cm y^{-1}. During the last 1.5 cal ka BP, SAR decreased to 0.01 cm y^{-1} (Fig. 4). The amount of IRD was the highest prior to ~ 2.7 cal ka BP, reaching up to 83 grains g^{-1}. After 2.7 cal ka BP, the amount of IRD was relatively stable and did not exceed 18 grains g^{-1}. The flux of IRD

slightly decreased with time to 0.37 grains g^{-1} cm^{-1}, except for one peak ~ 2.6 cal ka BP, when it reached 0.8 grains g^{-1} cm^{-1} (Fig. 4).

The mean grain size of the 0-63-μm fraction had its highest value (5.8 φ) at ~ 2.7 cal ka BP (Fig. 4) and after 2.4 cal ka BP a slight but continuous reduction in the mean 0-63-μm grain size was noted. The minimum grain size (6.23 φ) was recorded at the top of the core.

4.2 Stable isotopes

The $\delta^{18}O$ values were relatively stable prior to ~ 2.7 cal ka BP, varying slightly between 3.55‰ and 3.69‰ vs. VPDB. Between ~ 2.7 and 1.5 cal ka BP, $\delta^{18}O$ showed the strongest variation, with values ranging from 3.28‰ to 3.77‰ vs. VPDB. After ~ 1.5 cal ka BP, $\delta^{18}O$ became slightly lighter and varied between 3.43‰ and 3.64‰ vs. VPDB except for one peak noted in the uppermost layer of the core, where $\delta^{18}O$ reached 3.87‰ vs. VPDB (Fig. 4). $\delta^{13}C$ values varied throughout the core with slightly lighter values, ranging from 0.92‰ to 1.12‰ vs. VPDB prior to ~ 2.7 cal ka BP. $\delta^{13}C$ values reaching up to 1.46‰ vs. VPDB were noted between ~ 2.7 and ~ 1.5 cal ka BP and gradually decreased from ~ 1.5 cal ka BP to the present, reaching 0.81‰ vs. VPDB at the top of the core (Fig. 4).

4.3 Fossil foraminifera

A total of 8647 fossil foraminifera specimens belonging to 47 species were identified (Supplement 1; Supplementary Fig. 1). The foraminiferal assemblages were dominated by calcareous taxa which account for 62–98% of the foraminifera specimens except in the uppermost layer of the core, where the percentage of calcareous foraminifera decreased to 44% (Fig. 4). There were few peaks of agglutinated foraminifera noted at 2.0 cal ka BP, 1.8 cal ka BP and on the sediment surface, where the percentages reached 37%, 37% and 66%, respectively (Fig. 4). The number of foraminiferal individuals varied from 156 to 2610 ind. g^{-1} and the lowest abundances were observed prior to ~ 2.7 cal ka BP (Fig. 4). A short-term decrease in the foraminiferal abundance was observed between 2.1 and 1.9 ka BP, with values reaching as low as 304 ind. g^{-1}. The abundance maxima were noted at 2.3, 1.5, and 0.6 ka BP, with values reaching 2524 ind. g^{-1}, 2584 ind. g^{-1}, and 2610 ind. g^{-1}, respectively. The foraminiferal flux was low and relatively stable throughout the core with values that did not exceed 1 ind cm^{-2} y^{-1}, except for two peaks at 2.3 and 1.5 ka BP, when the flux reached 2.2 ind cm^{-2} y^{-1} (Fig. 4).

The most abundant species was *Cassidulina reniforme*, with densities reaching up to 900 ind g^{-1}. The other species that constituted the majority of the foraminiferal assemblage

were *Bucella frigida*, *Cibicidoides lobatulus*, *Elphidium excavatum*, *Islandiella* spp, *Melonis barleeanum*, and *Nonionellina labradorica* The abundances of dominant species followed a general trend with maxima ~ 2.3 cal ka BP and after ~ 1.7 cal ka BP and minima prior to ~ 2.7 cal ka BP and between 2.3 and 1.7 cal ka BP. (Fig. 5).

The foraminiferal assemblage prior to ~ 2.7 cal ka BP was codominated by *Nonionellina labradorica* and *Melonis barleeanum*, which are species that are considered to be indicators of AW inflow and/or frontal zones, and glaciomarine taxa, primarily *Cassidulina reniforme* and *Elphidium excavatum*, which together accounted for up to 60% of the foraminiferal abundance (Fig. 5). After ~ 2.7 cal ka BP, there were AW/frontal zone indicator peaks recorded at 2.4 and 1.8 cal ka BP, where the percentages increased to 33%, and 28% of the total abundance. The period between ~ 2.4 cal ka BP and ~ 1.8 cal ka BP was characterized by an increase in the percentage of sea-ice indicators (*B. frigida* and *Islandiella* spp), which accounted for up to 25% of the total abundance, and by a short-term peak in the glaciomarine taxa, which accounted for up to 49% of foraminiferal assemblage between 2.5 and 2.1 cal ka BP. A decrease in the relative abundance of glaciomarine species was observed after ~ 0.5 cal ka BP and was followed by an increase in the AW/frontal zone indicators and a single peak in the percentage of bottom current indicators, which reached 42% and 19%, respectively (Fig. 5).

4.4 Foraminiferal aDNA sequences

A total of 1,499,889 foraminiferal DNA sequences were clustered into 263 OTUs, and 20 remained unassigned. The remaining OTUs were assigned to Globigerinida (5 OTUs), Robertinida (1 OTU), Rotaliida (49 OTUs), Textulariida (18 OTUs), Monothalamea (163 OTUs), and Miliolida (7 OTUs). The majority of sequences belonged to Monothalamea (60%) and Rotaliida (31%) (Supplement 2; Supplementary Fig. 2). Herein, we focus on Monothalamea, which is the dominant component of the foraminiferal aDNA record.

The most important components of the monothalamous assemblage were *Micrometula* sp., *Cylindrogullmia* sp., *Hippocrepinella hirudinea*, *Ovammina* sp., *Nemogullmia* sp., *Tinogullmia* sp., *Cedhagenia saltatus*, undetermined allogromiids belonging to clades A and Y (herein called "allogromiids"), and sequences belonging to taxa known exclusively from environmental sequencing (herein called "environmental clades"). The sequences belonging to allogromiids were present throughout the core, accounting for 16–31.7% of all the foraminiferal sequences, except during the intervals from ~ 4.0 to 2.4 cal ka BP, and ~ 1.7 cal ka BP, when contribution of allogromiid sequences decreased to less than 10% (Fig. 6). The

majority of the allogromiids belonged to clade Y, which accounted for up to 100% of the allogromiid sequences, except for the two peaks at 1.6–1.7 cal ka BP and 2.4–2.6 cal ka BP, when the majority of allogromiid sequences belonged to clade A. Also, allogromiids belonging to Clade I were noted at ~ 2.4 cal ka BP, where they made up 0.88% of allogromiid sequences (Fig. 7).

The periods prior to ~ 2.4 cal ka BP and ~ 1.7 cal ka BP were marked by the disappearance of sequences belonging to *C. saltatus*, *Nemogullmia* sp., and the environmental clades, followed by an increase in the percentages of sequences belonging to *Micrometula* sp., *Ovammina* sp., *Tinogullmia* sp., *Shepheardella* sp. and *Cylindrogullmia* sp. (Fig. 6).

4.5 Diatom aDNA sequences

A total of 824,697 diatom DNA sequences were clustered into 221 OTUs (Supplement 3; Supplementary Figure 3). The most abundantly sequenced diatom taxa were *Thalassiosira* spp, which made up 61.1 % of diatom sequences. Other abundantly sequenced taxa were *Chaetoceros* sp. and *T. antarctica*, which made up 8.5% and 11.5% of sequences. The sequences of *Thalassiosira* sp were most abundant between ~ 2.2 cal ka BP and ~ 1.9 cal ka BP, accounting for up to 85% of all diatom sequences. The lowest percentage (14%) of *Thalassiosira* sp. was recorded ~ 0.4 cal ka BP. Sequences assigned to *T. antarctica* were recorded throughout the core and their percentages were the highest ~ 3.3 and ~ 2.6 cal ka BP, reaching up to 13% and 19%, respectively (Fig. 8). Sequences of *T. hispida* were also noted throughout the core and constitute 4.7% of diatom sequences in the uppermost layer. In the remaining samples, *T. hispida* sequences did not exceed 1%. The percentage of sequences of *Chaetoceros* sp. decreased downcore, from 76% at the surface to less than 1% at the bottom of the core (Fig. 8). .*Navicula* sp. constituted an important part of diatom assemblage ~3.3 cal ka BP and ~1.9 cal ka BP, accounting for up to 25.5% and 10% of all diatom sequences, respectively. In the remaining samples, its abundance did not exceed 5% (Fig. 8).

6. Discussion

The ST_1.5 age model is based on the linear interpolation between the four dates, so the age control of the core should be treated with caution. However , the good correlation with other records from the region (e.g., Sarnthein et al., 2003, Rasmussen and Thomsen, 2014b) supports the ST_1.5 age model. The multiproxy record from Storfjorden revealed several intervals of pronounced environmental changes. The major environmental shifts occurred at ~ 2.7, 2.3 and 1.7 cal ka BP, what correlated well with the temperature minimum (2.7 cal ka

BP) and maxima (2.3 and 1.7 cal ka BP) recorded in the GISP2 core (Grootes & Stuiver, 1997) and 23258 core (Sarnthein et al., 2003).

6.1. The period from 4 cal ka BP to 2.7 cal ka BP

During the period prior to ~ 2.7 cal ka BP, the ST_1.5 sedimentary record displayed elevated and variable IRD delivery and coarsening of the 0-63-μm sediment fraction (Fig. 4). These results are in agreement with the record from Storfjordrenna (Łącka et al., 2015), where peaks in IRD were noted during the Neoglacial and were attributed to increased iceberg rafting due to fluctuations in the glacial fronts (e.g. Forwick et al., 2010). Coarser 0-63 μm may suggest winnowing of fine grained sediment, however, foraminiferal fauna showed no clear response for sediment removal.

The ST_1.5 foraminiferal assemblage was dominated by glacier-proximal fauna (primarily *C. reniforme*) and indicators of frontal zones (primarily *M. barleeanum*; Fig. 5). The presence of *C. reniforme* and *M. barleeanus* is linked to cooled and salty AW (e.g., Hald and Steinsund, 1996; Jernas et al., 2013). Moreover, these species are also associated with the presence of phytodetritus, which may be related to the delivery of fresh organic matter observed in frontal zones and/or near the sea-ice edge (Jennings et al., 2004). Relatively light $\delta^{13}C$ (Fig. 4), followed by the maximum percentage of sea-ice species *Thalassiosira antarctica* (cf Ikävalko, 2004; Fig. 8) may indicate primary production associated with the presence of sea-ice and/or periodic inflow of ArW

The typical response of a foraminiferal community to high trophic resources is an increase in diversity and standing stock (Wollenburg and Kuhnt, 2000). According to our data, the foraminiferal community showed no clear signs of increased productivity, as the abundance and flux of foraminifera were low prior to ~ 2.7 cal ka BP (Fig. 4). Similarly, Rasmussen and Thomsen (2015) noted a decrease in concentration of benthic foraminifera in Storfjorden at that time, which was attributed to the more extensive seasonal sea-ice cover. Also, Knies et al. (2017) suggested a variable sea-ice cover extent and a fluctuating sea-ice margin in Storfjorden prior to ~ 2.8 cal ka BP. In contrast, our data may suggest the presence of high-energy environment during the interval prior to ~ 2.7 cal ka BP, what may be the major factor limiting the development of the foraminiferal community. However, low sampling resolution during that period precluded making any general conclusion and the latter assumption should be confirmed by further studies.

6.2 The period after 2.7 cal ka BP. Episodes of AW inflow at ~ 2.3 and 1.7 cal ka BP.

The environmental conditions in central Storfjorden changed noticeably after ~ 2.7 cal ka BP. The increase in SAR was followed by a gradual decrease in the 0-63-μm fraction and a decrease in the IRD delivery after ~ 2.7 cal ka BP (Fig. 4). The 10-fold increase in SAR resulted most likely from the intensive supply of turbid meltwater from advancing glaciers and consequent intensive sedimentation. Moreover, the accumulation of fine sediment may also be enhanced by the slowdown of the bottom currents, indicated by the finer 0-63-μm sediment fraction (Fig. 4). On the other hand, a decrease in IRD delivery may suggest that the central Storfjorden was not impacted by iceberg rafting at that time. In contrast, Rasmussen and Thomsen (2015) suggested glacial advance, followed by intensive ice rafting and meltwater delivery to Storfjorden at that time. According to Knies et al. (2017), the distinct surface water cooling during the Neoglacial provides a prerequisite for the presence of more extensive sea-ice cover; therefore inner Storfjorden was covered by densely packed sea ice between ~ 2.8 and 0.5 cal ka BP. Therefore, the decreasing IRD in the ST_1.5 core may result from the presence of a sea-ice cover that reduced iceberg rafting while the majority of coarse-grained material settled in the proximity of the glacial fronts. Similar conclusions have been stated by Forwick and Vorren (2009) and Forwick et al. (2010), who assumed that the enhanced formation of sea ice along the West Spitsbergen coast trapped icebergs inside the Isfjorden system.

Both heavy ice cover and meltwater delivery may limit light penetration in the water and therefore suppress primary production and organic matter export to the bottom. However, the foraminiferal fauna in central Storfjorden revealed more than a 10-fold increase in flux and abundance followed by short-term fluctuations after ~ 2.7 cal ka BP (Fig. 3); this may suggest favorable conditions for foraminiferal growth. The major peaks in the total foraminiferal abundance (Fig. 4) followed by peaks in the percentage of AW foraminiferal indicators (Fig. 5) were noted ~ 2.3 cal ka BP and ~ 1.7 cal ka BP. These peaks were associated with the occurrence of sequences of *T. hispida* (Fig. 8), a diatom species characteristic of subpolar and temperate regions (Katsuki et al., 2009). These results are in accordance with the findings of Sarntheim et al. (2003), who reported two intervals of the remarkably warmer sea surface on the western continental margin of the Barents Sea at ~ 2.2 and ~ 1.6 cal ka BP, which was attributed to short-term pulses of warm AW advection. Moreover, the western Spitsbergen continental margin experienced periods of a rapidly advancing and retreating sea-ice margin during the Neoglacial, caused by a temporarily strengthened AW inflow and/or changes in the atmospheric circulation patterns (Müller et al., 2012). Our foraminiferal and diatom aDNA records confirm the presence of AW intrusions

that may cause an episodic breakup of sea ice cover and permits primary production and development of benthic biota, including foraminifera.

Knies et al. (2017) have suggested that the pulses of advected AW did not influence the persistent sea-ice cover in Storfjorden between ~ 2.8 and 0.5 cal ka BP. However, the ST_1.5 foraminiferal record indicates that central Storfjorden was not constantly covered by sea ice at that time. A more reasonable scenario is surface water cooling and periodic melting and freezing of the sea surface and consequent production of brines, which launched convective water mixing and nutrient resupply to the surface, thereby stimulating primary production (Łącka et al., *in prep.*). The presence of diatom aDNA sequences throughout the Neoglacial (Fig. 8) may suggest continuous primary production. It is likely that pulses of AW inflow at 2.3 cal ka BP and 1.7 cal ka BP induced melting of the ice cover, leading to the formation of ice-free areas and highly productive ice marginal zones. This conjecture may be supported by peaks in the light $\delta^{18}O$ in benthic foraminiferal tests, the maxima of the foraminiferal flux (Fig. 4) and peaks in the abundance of species associated with highly productive environments such as *M. barleeanum* and *N. labradorica* (Fig. 5). Similarly, the foraminiferal flux and abundance were elevated and slightly variable after ~ 1.7 cal ka BP. The foraminiferal assemblage was codominated by AW/frontal zone indicators and glaciomarine species (Fig. 5) at that time, which may suggest rather ameliorated environmental conditions. However, the response of benthic foraminifera assemblage to the pulses of AW at ~ 2.3 cal ka BP and ~ 1.7 cal ka BP is slightly different. The dominant components of foraminiferal assemblage at ~ 2.3 cal ka BP were *M. barleeanum* and *E. excavatum*, while at ~ 1.7 cal ka BP, *N. labradorica* and *C. reniforme* reached higher percentages. The major difference in environmental conditions between these two "AW episodes" was noticeably coarser 0-63 μm sediment fraction noted at ~ 2.3 cal ka BP, what may indicate more intensive winnowing and consequent sediment sorting, what creates favorable conditions for development of highly opportunistic species, such as *E. excavatum*, which reached its' maximum flux and percentage at that time. In contrast, the interval between 2.3 and 1.7 cal ka BP featured variable $\delta^{13}C$ and $\delta^{18}O$ followed by a decrease in the foraminiferal flux and abundance (Fig. 4). The foraminiferal assemblage at this time was dominated by glaciomarine and sea-ice taxa (Fig. 5), which indicate more severe environmental conditions with extensive ice cover and suppressed productivity. The sea-ice formation led to a more intensive release of brines and consequently, stronger bottom current activity reflected in a minor increase in 0-63 μm fraction and slight increase in the percentage of *C. lobatulus*, which is considered to be a bottom current indicator (Fig. 5).

The above-described environmental changes were also reflected in the aDNA record of monothalamous foraminifera. During the time intervals of 2.2–1.9 cal ka BP and 1.3–0.4 cal ka BP, monothalamous foraminifera was dominated by allogromiids belonging to clade Y, *Nemogullmia* sp., *C. saltatus* and monothalamids belonging to so called "environmental clades" (Fig. 6). Allogromiids are not a coherent taxonomic group but are scattered between several monothalamous clades (Gooday 2002; Pawlowski et al., 2002). Considerable part of the allogromiid sequences in the ST_1.5 core belong to clade Y (Fig. 7), which is primarily composed of taxa known only from environmental sequencing. Sequences belonging to clade Y have previously been noted in modern sediments in the Spitsbergen fjords (Pawłowska et al., *in prep.*). Moreover, clade Y has been abundantly sequenced in the coastal areas off Scotland, characterized by high levels of environmental disturbances (Pawlowski et al., 2014a); this might suggest its high tolerance to environmental stress. In addition, so called "environmental clades" comprised of monothalamous taxa known exclusively from environmental sequencing (Lecroq et al., 2011) and may belong to novel, undescribed foraminiferal lineages (Pawlowski et al., 2014b). *C. saltatus* was recently found by Gooday et al. (2011) in the Black Sea and until recently, little has been known about its environmental tolerances; however, its occurrence in areas with high levels of pollution suggests that it is an opportunistic species with a high tolerance to environmental disturbances. Specimens of *Nemogullmia* were also found in the Spitsbergen fjords (Gooday et al., 2005; Majewski et al., 2005); however, data on its abundance and distribution may be incomplete due to the degradation of its fragile, organic-walled tests. The abovementioned taxa nearly disappeared during episodes of enhanced AW inflow ~ 2.4 cal ka BP and ~ 1.7 cal ka BP, and the monothalamous assemblage was dominated at that time by *Micrometula* sp., *Ovammina* sp., *Shepheardella* sp., *Tinogullmia* sp., *Cylindrogullmia* sp., and allogromiids belonging to clade A (Fig. 6; Fig. 7). All these taxa have recently been observed in the fjords of Svalbard (e.g. Gooday et al., 2005; Majewski et al., 2005; Sabbattini et al., 2007; Pawłowska et al., 2014). *Cylindrogullmia* sp. commonly been found in the inner parts of the fjords (Gooday et al., 2005). Hughes and Gooday (2004) suggest that *Cylindrogullmia* sp. is an infaunal species that normally resides in deeper sediment layers of sediment. *Micrometula* sp. was among the abundantly found organic-walled allogromiids in glacier-proximal sites off Novaya Zemlya (Korsun & Hald, 1998; Korsun et al., 1995) and Svalbard (Korsun & Hald, 2000; Gooday et al., 2005; Pawłowska et al., 2014). Moreover, *Cylindrogullmia* and *Micrometula* are dependent on the presence of fresh phytodetritus (Alve, 2010). *Ovammina* sp. feeds on diatoms and other forms of microalgae (Goldstein & Alve, 2011). Similarly, the presence of

Tinogullmia is largely controlled by the presence of organic material on the seafloor. High concentrations of *Tinogullmia* have been found in coastal (Cornelius & Gooday, 2004) and deep-sea regions (Gooday, 1993) within phytodetrital aggregates.

The taxa that dominated the monothalamous assemblage during warm intervals seem to be responsive to the delivery of organic matter and may flourish during phytoplankton blooms associated with the settling of organic matter (e.g., Alve, 2010; Sabbattini et al., 2012, 2013). The pulses of AW inflow that are associated with sea-ice melting stimulated phytoplankton blooms and organic matter supply to the bottom. The enhanced primary productivity supported the development of an organic matter-dependent monothalamous community. Conversely, the colder phases of the Neoglacial were characterized by heavy and densely packed sea ice resulting in limited productivity (Knies et al., 2017). Therefore, the monothalamous assemblage was less diverse and was dominated by more opportunistic taxa.

The decrease in the percentage of foraminiferal sea-ice indicators noted at ~ 1.7 cal ka BP and after ~ 1.5 cal ka BP suggests a gradually diminishing sea-ice coverage in Storfjorden (Fig. 5). Modern-like conditions were established in Storfjorden ~ 0.5 cal ka BP, with seasonally variable sea-ice cover resulting in intensified but variable polynyal activity (Rasmussen and Thomsen, 2014b; Knies et al., 2017). The IP_{25} records from the western Spitsbergen shelf indicate variable sea-ice conditions during the last 2 ka (Cabedo-Sanz and Belt, 2016). Moreover, the majority of diatom aDNA sequences after ~ 0.5 cal ka BP belonged to *Chaetoceros* sp., a taxa that is observed in surface waters and is almost entirely absent under sea ice (Różańska et al., 2008). Moreover, high abundances of *Chaetoceros* are often associated with highly productive surface waters (Cremer, 1999), which indicate declining sea-ice cover (Cabedo-Sanz and Belt, 2016). However, the aDNA record of the monothalamous foraminifera ~ 0.4 cal ka BP displayed relatively high percentages of taxa that dominated during colder intervals of the Neoglacial (Fig. 6); this may be related to the recovery from the Little Ice Age and consequently, temporarily deteriorated environmental conditions (D'Andrea et al., 2012). However, further studies are required to confirm the latter conclusion.

6.3 Paleoceanographic implications

Our record revealed two-phase Neoglacial, with a major shift in environmental conditions at ~ 2.7 cal ka BP. According to the ST_1.5 record, the Neoglacial in Storfjorden was not a constantly cold period, but comprised alternate, short-term cooling and warming periods, associated with variability in sea-ice coverage and productivity. There is various

evidence of a shift in environmental conditions in the Nordic Seas region in mid-Neoglacial. Alkenone record from the Norwegian Sea revealed a significant drop of sea surface temperature at 2.7 cal ka BP (Calvo et al., 2002). Risebrobakken et al. (2010) recorded a change in oceanographic conditions in the SW Barents Sea ca. 2.5 cal ka BP, followed by the episodes of reduced surface and subsurface salinity after 2.5 cal ka BP, what was attributed to the expansion of coastal waters and the occurrence of more sea-ice.

Moreover, our evidence of the presence of AW in Storfjorden during the Neoglacial supported previous suggestions that AW inflow during the late Holocene was strong enough to reach also the eastern coasts of Svalbard (e.g., Łącka et al., 2015). Moreover, Sarnthein et al. (2003) postulated pulses of AW inflow to the western Barents Sea shelf at 2.2 and 1.6 cal ka BP. According to Perner et al. (2015), the Neoglacial delivery of chilled AW to the Nordic Seas culminated between 2.3 and 1.4 cal ka BP. Also, Rasmussen et al. (2014a) and Jernas et al (2013) recorded slightly warmer and less glacial conditions during the last 2 ka on the western Spitsbergen shelf.

7. Conclusions

The ST_1.5 multiproxy record revealed that the environmental variability in Storfjorden during the Neoglacial was steered controlled primarily by the interplay between AW and ArW and changes in the sea-ice cover. The molecular record supports and complements sedimentary and microfossil records, which indicate that major changes in the environmental conditions in Storfjorden occurred at ~ 2.7 cal ka BP. The general cooling at the early phase of the Neoglacial initiated conditions for the formation of extensive sea-ice cover. The latter part of the Neoglacial (after ~ 2.7 cal ka BP) was characterized by alternating short-term cooling and warming periods. Warming was associated with pulsed inflows of AW and sea-ice melting, which may stimulate phytoplankton blooms and organic matter supply to the bottom. The cold phases were characterized by heavy and densely packed sea ice resulting in limited productivity.

Moreover, the aDNA diatom record supports the conclusion that primary production took place continuously during the Neoglacial, regardless of the sea-ice conditions. The early phase of the Neoglacial was characterized by the presence of diatom taxa associated with sea ice, whereas the present-day diatom assemblage was dominated by *Chaetoceros* spp, a taxa characteristic of open water.

The aDNA record of monothalamous foraminifera is in agreement with the microfossil record and revealed the timing of the major pulses of AW at 2.3 and 1.7 cal ka BP. The AW

inflow was marked by an increase in the percentage of sequences of monothalamous taxa associated with the presence of fresh phytodetritus. The monothalamous assemblage during cold intervals was less diverse and was dominated by monothalamous foraminifera known only from environmental sequencing.

Author contribution

MZ and Jan P designed the study. Joanna P, MŁ and MZ collected the sediment core. MŁ and MK performed the sedimentological and micropaleontological analyses. Joanna P performed the molecular analyses and prepared the manuscript with contributions from all co-authors.

Acknowledgements

The study was supported by the National Science Centre grants no. 2015/19/D/ST10/00244 and 2016/21/B/ST10/02308, and Swiss National Science Foundation grant no. 31003A_179125. The Authors would like to thank two anonymous Reviewers for constructive comments that helped to improve the manuscript.

References

Alve, E.: Benthic foraminiferal responses to absence of fresh phytodetritus: A two – year experiment, Mar. Micropaleontol., 76, 67-76, https://doi.org/10.1016/j.marmicro.2010.05.003, 2010.

Altschul, S.F., Gish, W., Miller, W., Myers, E.W., Lipman, D.J.: Basic local alignment search tool. J. Mol. Biol. 215, 403-410, https://doi.org/10.1016/S0022-2836(05)80360-2, 1990.

Andersen, C., Koç, N., Moros, M.: A highly unstable Holocene climate in the subpolar North Atlantic: evidence from diatoms, Quat. Sci. Rev., 23, 2155-2166, https://doi.org/10.1016/j.quascirev.2004.08.004, 2004.

Årthun, M., Ingvaldsen, R.B., Smedsrud, L.H., Schrum, C.: Dense water formation and circulation in the Barents Sea, Deep Sea Res. Part I: Oceanogr. Res. Pap., 58, 801-817, https://doi.org/10.1016/j.dsr.2011.06.001, 2011.

Berger, A.L.: Long-term variations of daily insolation and quaternary climatic changes, J. Atmos. Sci., 35, 2362-2367, https://doi.org/10.1175/1520-0469(1978)035<2362:LTVODI>2.0.CO;2 1978.

Blott, S.J., Pye, K.: GRADISTAT: a grain size distribution and statistics package for the analysis of unconsolidated sediments, Earth Surf. Process. Landf., 26, 1237 – 1248, https://doi.org/10.1002/esp.261, 2001.

Cabedo-Sanz, P., Belt, S.T.: Seasonal sea ice variability in eastern Fram Strait over the last 2000 years, Arktos, 2, 22, doi: 10.1007/s41063-016-0023-2, 2016.

Boere, A.C., Abbas, B., Rijpstra, W.I.C., Versteegh, G.J., Volkman, J.K., Sinninghe Damsté, J.S., Coolen, M.J.L.: Late-Holocene succession of dinoflagellates in an Antarctic fjord using a multi-proxy approach: paleoenvironmental genomics, lipid biomarkers and palynomorphs, Geobiol., 7, 265-281, https://doi.org/10.1111/j.1472-4669.2009.00202.x, 2009.

Calvo, E., Grimalt, J., Jansen, E.: High resolution U_{37}^{K} sea surface temperature reconstruction in the Norwegian Sea during the Holocene. Quat. Sci. Rev., 21, 1385-1394, https://doi.org/10.1016/S0277-3791(01)00096-8, 2002.

Cornelius, N., Gooday, A.J.: 'Live' (stained) deep-sea benthic foraminiferans in the western Weddell Sea: trends in abundance, diversity and taxonomic composition along a depth transect, Deep Sea Res. II, 51, 1571-1602, https://doi.org/10.1016/j.dsr2.2004.06.024, 2004.

Cremer, H.: Distribution patterns of diatom surface sediment assemblages in the Laptev Sea (Arctic Ocean), Mar. Micropaleontol., 38, 39-67, https://doi.org/10.1016/S0377-8398(99)00037-7, 1999.

D'Andrea, W.J., Vaillencourt, D.A., Balascio, N.L., Werner, A., Roof, S.R., Retelle, M., Bradley, R.S.: Mid Little Ice Age and unpredecented recent warmth in an 1800 year lake sediment record from Svalbard, Geology, 40, 1007-1010, https://doi.org/10.1130/G33365.1**,** 2012.

Dufresne, Y., Lejzerowicz, F., Apotheloz Perret-Gentil, L., Pawlowski, J., Cordier, T.: SLIM: a flexible web application for the reproducible processing of environmental DNA metabarcoding data. BMC Bioinformatics, 20, 88, https://doi.org/10.1186/s12859-019-2663-2, 2019.

Forwick, M., Vorren, T.O.,: Late Weichselian and Holocene sedimentary environments and ice rafting in Isfjorden, Spitsbergen, Palaeogeogr. Palaeoclimatol. Palaeoecol. 280, 258-274, https://doi.org/10.1016/j.palaeo.2009.06.026, 2009.

Forwick, M., Vorren, T.O., Hald, M., Korsun, S., Roh, Y., Vogt, C., Yoo, K.-C.: Spatial and temporal influence of glaciers and rivers on the sedimentary environment in Sassenfjorden and Tempelfjorden, Spitsbergen. In: Geological Society, London, Special Publications, vol 344 (1): 163-193, https://doi.org/10.1144/SP344.13, 2010.

Geyer, F., Fer, I., Smedsrud, L. H.: Structure and forcing of the overflow at the Storfjorden sill and its connection to the Arctic coastal polynya in Storfjorden, Ocean Sci., 6(1), 401-411, https://doi.org/10.5194/os-6-401-2010, 2010.

Goldstein, S.T., Alve, E.: Experimental assembly of foraminiferal communities from coastal propagule banks, Mar. Ecol. Prog. Ser. 437, 1-11, https://doi.org/10.3354/meps09296, 2011.

Gooday, A.J.: Deep-sea benthic foraminiferal species which exploit phytodetritus: Characteristic features and controls on distribution, Mar. Micropaleontol., 22, 187-205, https://doi.org/10.1016/0377-8398(93)90043-W, 1993.

Gooday, A.J.: Organic-walled allogromiids: aspects of their occurrence, diversity and ecology in marine habitats, J. Foramin. Res., 32, 384-399, https://doi.org/10.2113/0320384, 2002.

Gooday, A.J., Bowser, S.S., Cedhagen, T., Cornelius, N., Hald, M., Korsun, S., Pawłowski, J.: Monothalamous foraminiferans and gromiids (Protista) from western Svalbard: A preliminary survey, Mar. Biol. Res., 1, 290 – 312, https://doi.org/10.1080/17451000510019150, 2005.

Gooday, A.J., Anikeeva, O.V., Pawlowski, J.: New genera and species of monothalamous Foraminifera from Bataclava and Kazach'ya Bays (Crimean Peninsula, Black Sea), Mar. Biodiv., 41, 481-494, https://doi.org/10.1007/s12526-010-0075-7, 2011.

Grootes, P.M., and M. Stuiver. 1997. Oxygen 18/16 variability in Greenland snow and ice with 10^{-3} to 10^{-5}-year time resolution. J. Geophys. Res., 102, 26455-26470, https://doi.org/10.1029/97JC00880, 1997.

Haarpainter, J., Gascard, J.C., Haugan, P.M.: Ice production and brine formation in Storfjorden, Svalbard, *J. Geophys. Res. 106 C7*, 14 001–14 013, https://doi.org/10.1029/1999JC000133, 2001.

Hald, M. Steinsund, P.I.: Benthic foraminifera and carbonate dissolution in the surface sediments of the Barents and Kara Seas, Berichte zur Polarforschung, 212, 285–307, 1996.

Hansen, J., Hanken, N.-M., Nielsen, J.K., Nielsen, J.K., Thomsen, E.: Late Pleistocene and Holocene distribution of *Mytilus edulis* in the Barents Sea region and its paleoclimatic implications, J. Biogeogr, 38, 1197-1212, https://doi.org/10.1111/j.1365-2699.2010.02473.x, 2011.

Hughes, J.A., Gooday, A.J.: Associations between living benthic foraminifera and dead tests of Syringammina fragilissima (Xenophyophorea) in the Darwin Mounds region (NE Atlantic), Deep Sea Res. Part I: Oceanographic Research Papers, 51, 1741-1758, https://doi.org/10.1016/j.dsr.2004.06.004, 2004.

Ikävalko, J.: Checklist of unicellular and invertebrate organisms within and closely associated with sea ice in the Arctic regions. MERI – Report Series of the Finnish Institute of Marine Research, 52, Helsinki, Finland, Finnish Institute of Marine Research, 2004.

Jennings, A.E., Weiner, N.J., Helgadottir, G., Andrews, J.T.: Modern foraminiferal faunas of the southwestern to northern Iceland Shelf; oceanographic and environmental controls, J. Foramin. Res., 34, 180-207, https://doi.org/10.2113/34.3.180, 2004.

Jernas, P., Klitgaard Kristensen, D., Husum, K., Wilson, L., Koç, N.: Palaeoenvironmental changes of the last two millennia on the western and northern Svalbard shelf, Boreas, 42, 236-255, https://doi.org/10.1111/j.1502-3885.2012.00293.x, 2013.

Katsuki, K., Takahashi, K., Onodera, J., Jordan, R.W., Suto, I.: Living diatoms in the vicinity of the North Pole, summer 2004, Micropaleontol. 55, 137-170, 2009.

Killworth, P.D.: Deep convection in the World Ocean, Rev. Geophys., 21, 1-26, doi:10.1029/RG021i001p00001, 1983.

Knies, J., Pathirana, I., Cabedo-sanz, P., Banica, A., Fabian, K., Rasmussen, T.L., Forwick, M., Belt, S.: Sea-ice dynamics in an Arctic coastal polynya during the past 6500 years, Arktos, 3, 1, https://doi.org/10.1007/s41063-016-0027-y, 2017.

Korsun, S., Hald, M.: Modern benthic Foraminifera off Novaya Zemlya tidewater glaciers, Arctic and Alpine Research, 30, 61-77, https://doi.org/10.1080/00040851.1998.12002876, 1998.

Korsun, S., Hald, M.: Seasonal dynamics of benthic foraminifera in a glacially fed fjord of Svalbard, European Arctic, J. Foramin. Res., 30, 251-271, https://doi.org/10.2113/0300251, 2000.

Korsun, S., Pogodina, I.A., Forman, S.L., Lubinski, D.J.: Recent foraminifera in glaciomarine sediments from three arctic fjords of Novaja Zemlja and Svalbard, Polar Res., 14, 15 – 31, https://doi.org/10.1111/j.1751-8369.1995.tb00707.x, 1995.

Lejzerowicz, F., Esling, P., Majewski, W., Szczuciński, W., Decelle, J., Obadia, C., Martinez Arbizu, P., Pawlowski, J.: Ancient DNA complements microfossil record in deep-sea subsurface sediments. Biol. Lett., 9, 20130283, https://doi.org/10.1098/rsbl.2013.0283, 2013.

Lecroq B., Lejzerowicz F., Bachar D., Christen R., Esling P., Baerlocher L., Østerås M., Frinelli L., Pawlowski J.: Ultra-deep sequencing of foraminiferal microbarcodes unveils hidden richness in deep-sea sediments, PNAS, 108:13177-82, https://doi.org/10.1073/pnas.1018426108, 2011.

Lydersen, C., Nøst, O., Lovell, P., McConell, B., Gammelsrød, T., Hunter, C., Fedak, M., Kovacs, K.: Salinity and temperature structure of a freezing Arctic fjord – monitored by white

whales (Delphinapterus leucas), Geophys. Res. Lett., 29, 2119, https://doi.org/10.1029/2002GL015462, 2002.

Łącka, M., Zajączkowski, M., Forwick, M., Szczuciński, W.: Late Weichselian and Holocene palaeoceanography of Storfjordrenna, southern Svalbard, Clim. Past, 11, 587-603, https://doi.org/10.5194/cp-11-587-2015, 2015.

Mahé, F., Rognes T., Quince C., de Vargas, C., Dunthorn, M.: Swarm: robust and fast clustering method for amplicon-based studies, Peer J, 2, e593, doi: 10.7717/peerj.593, 2014.

Majewski, W., Pawłowski, J., Zajączkowski, M.: Monothalamous foraminifera from West Spitsbergen fjords: a brief overview, Polish Polar Res., 26(4), 269-285, 2005.

Majewski, W., Szczuciński, W., Zajączkowski, M.: Interactions of Arctic and Atlantic water-masses and associated environmental changes during the last millennium, Hornsund (SW Svalbard). Boreas, 38, 529-544, https://doi.org/10.1111/j.1502-3885.2009.00091.x, 2009.

Mangerud, J., Bondevik, S., Gulliksen, S., Hufthammer, A.K., Høseter, T.: Marine ^{14}C reservoir ages for 19th century whales and mollusks from the North Atlantic, Quat. Sci. Rev., 25, 3228-3245, https://doi.org/10.1016/j.quascirev.2006.03.010, 2006.

Martrat, B., Grimalt, J.O., Villanueva, J., van Kreveld, S., Sarntheim, M.: Climatic dependence of the organic matter contributions in the north eastern Norwegian Sea over the last 15,000 years, Org. Geochem., 34, 1057-1070, https://doi.org/10.1016/S0146-6380(03)00084-6, 2003.

Müller, J., Werner, K., Stein, R., Fahl, K., Moros, M., Jansen, E.: Holocene cooling culminates in sea ice oscillations in Fram Strait. Quaternary Science Reviews, 47,1–14, https://doi.org/10.1016/j.quascirev.2012.04.024, 2012.

Nilsen, F., Cottier, F., Skogseth, R., Mattson, S.: Fjord-shelf exchanges controlled by ice and brine production: The interannual variation of Atlantic Water in Isfjorden, Svalbard, Cont. Shelf Res. 28, 1838-1853, https://doi.org/10.1016/j.csr.2008.04.015, 2008.

Pawłowska, J., Lejzerowicz, F., Esling, P., Szczuciński, W., Zajączkowski, M., Pawlowski, J.: Ancient DNA sheds new light on the Svalbard foraminiferal fossil record from the last millennium, Geobiology, 12, 277-288, https.://doi.org/10.1111/gbi.12087, 2014.

Pawłowska, J., Zajączkowski, M., Łącka, M., Lejzerowicz, F., Esling, P., Pawlowski, J.: Palaeoceanographic changes in Hornsund Fjord (Spitsbergen, Svalbard) over the last millennium: new insights from ancient DNA, Clim. Past, 12, 1459-1472, https://doi.org/10.5194/cp-12-1459-2016, 2016.

Pawlowski, J., Holzmann, M., Berney, C., Fahrni, J., Cedhagen, T., Bowser, S.S.: Phylogeny of allogromiid Foraminifera inferred from SSU rRNA gene sequences, J. Foramin. Res., 32, 334-343, https://doi.org/10.2113/0320334, 2002.

Pawlowski, J., Esling, P., Lejzerowicz, F., Cedhagen, T., Wildings, T.A.: Environmental monitoring through protest next-generation sequencing metabarcoding: assessing the impact of fish farming on benthic foraminifera communities, Mol. Ecol. Res., 14, 1129-1140, doi: 10.1111/1755-0998.12261, 2014a.

Pawlowski, J., Lejzerowicz, F., Esling, P.: Next-generation environmental diversity surveys of foraminifera: Preparing the future, Biol. Bull., 227, 93-106, https://doi.org/10.1086/BBLv227n2p93, 2014b.

Perner, K., Moros, M., Lloyd, J.M., Jansen, E., Stein, R.: Mid to late Holocene strengthening of the East Greenland Current linked to warm subsurface Atlantic water, Quat. Sci. Rev., 129, 296-307, https://doi.org/10.1016/j.quascirev.2015.10.007, 2015.

Piechura, J.: Dense bottom waters in Storfjord and Storfjordrenna, Oceanologia, 38, 285-292, 1996.

Polyakov, I. V., Pnyushkov, A.V., Alkire, M.B., Ashik, I.M., Baumann, T.M., Carmack, E.C., Goszczko, I., Guthrie, J., Ivanov, V.V., Kanzow, T.T., Greater role for Atlantic inflows on sea-ice loss in the Eurasian Basin of the Arctic Ocean, Science, eaai8204, https://doi.org/10.1126/science.aai8204, 2017.

Quadfasel, D., Rudels, B., Kurz, K.: Outflow of dense water from a Svalbard fjord into the Fram Strait, Deep Sea Res., 35, 1143-1150, https://doi.org/10.1016/0198-0149(88)90006-4, 1988.

Rasmussen, T.L., Forwick, M., Mackensen, A.: Reconstruction of inflow of Atlantic Water to Isfjorden, Svalbard during the Holocene: Correlation to climate and seasonality, Mar. Micropaleontol., 94-95, 80-90, https://doi.org/10.1016/j.marmicro.2012.06.008, 2012.

Rasmussen, T.L., Thomsen, E., Skirbekk, K., Ślubowska-Woldengen, M., Klitgaard Kristensen, D., Koç, N.: Spatial and temporal distribution of Holocene temperature maxima in the northern Nordic seas: interplay of Atlantic-, Arctic- and polar water masses, Quat. Sci. Rev., 92, 280-291, https://doi.org/10.1016/j.quascirev.2013.10.034, 2014a.

Rasmussen, T. L., Thomsen, E.: Brine formation in relation to climate changes and ice retreat during the last 15,000 years in Storfjorden, Svalbard, 76-78°N, Paleoceanography, 29, 911–929, https://doi.org/10.1002/2014PA002643, 2014b.

Rasmussen, T.L., Thomsen, E.: Palaeoceanographic development in Storfjorden, Svalbard, during the deglaciation and Holocene: evidence from benthic foraminiferal records. Boreas, 44, 24–44, https://doi.org/10.1111/bor.12098, 2015.

Reimer, P. J., Bard, E., Bayliss, A., Beck, J. W., Blackwell, P. G., Bronk Ramsey, C., van der Plicht, J.: IntCal13 and Marine13 Radiocarbon Age Calibration Curves 0-50,000 Years Cal BP. Radiocarbon, 55(4), 1869-1887, https://doi.org/10.2458/azu_js_rc.55.16947, 2013.

Risebrobakken, B., Moros, M., Ivanova, E.V., Chistyakova, N., Rosenberg, R.: Climate and oceanographic variability in the SW Barents Sea during the Holocene, The Holocene, 20, 609-612, https://doi.org/10.1177/0959683609356586, 2010.

Rognes, T., Flouri, T., Nichols, B., Quince, C., Mahé, F.: VSEARCH: a versatile open source tool for metagenomics. Peer J, 4, e2584, https://doi.org/10.7717/peerj.2584, 2016.

Różańska, M., Poulin, M., Gosselin, M.: Protist entrapment in newly formed sea ice in the Coastal Arctic Ocean, J. Mar. Sys., 74, 887-901, https://doi.org/10.1016/j.jmarsys.2007.11.009, 2008.

Rudels, B., Korhonen, M., Schauer, U., Pisarev, S., Rabe, B., Wisotzki, A.: Circulation and transformation of Atlantic water in the Eurasian Basin and the contribution of the Fram Strait inflow branch to the Arctic Ocean heat budget, Prog. Oceanogr., 132, 128-152, https://doi.org/10.1016/j.pocean.2014.04.003, 2015.

Sarnthein, M., Van Kreveld, S., Erlenkeuser, H., Grootes, P.M., Kucera, M., Pflaumann, U., Schulz, M.: Centennial-to-millennial-scale periodicities of Holocene climate and sediment injections off the western Barents shelf, 75°N, Boreas, 32, 447-461, https://doi.org/10.1111/j.1502-3885.2003.tb01227.x, 2003.

Sabbattini, A., Morigi, C., Negri, A., Gooday, A.J.: Distribution and biodiversity of stained Monothalamous foraminifera from Tempelfjord, Svalbard, J. Foramin. Res., 37, 93-106, htttps://doi.org/ 10.2113/gsjfr.37.2.93, 2007.

Sabbattini, A., Bonatto, S., Bianchelli, S., Pusceddu, A., Danovaro, R., Negri A.: Foraminiferal assemblages and trophic state in coastal sediments of the Adriatic Sea, J. Mar. Syst., 105, 163-174, https://doi.org/10.1016/j.jmarsys.2012.07.009, 2012.

Sabbattini, A., Nardelli M.P., Morigi C., Negri, A.: Contribution of soft-shelled monothalamous taxa to foraminiferal assemblages in the Adriatic Sea, Acta Protozool., 52, 181-192, https://doi.org/10.4467/16890027AP.13.0016.1113, 2013.

Skogseth, R., Haugan, P.M., Haarpaintner, J.: Ice and brine production in Storfjorden from four winters of satellite and in situ observations and modeling, *J. Geophys. Res.*, *109*, C10008, https://doi.org/10.1029/2004JC002384, 2004.

Skogseth, R., Haughan, P.M., Jakobsson, M.: Watermass transformations in Storfjorden, Cont. Shelf Res., 25, 667-695, https://doi.org/10.1016/j.csr.2004.10.005, 2005.

Skogseth, R., Sandvik, A. D., Asplin, L.: Wind and tidal forcing on the meso-scale circulation in Storfjorden, Svalbard, Cont. Shelf Res., 27, 208-227, https://doi.org/10.1016/j.csr.2006.10.001, 2007.

Stuiver, M., Reimer, P.J.: Extended ^{14}C database and revised CALIB 3.0 ^{14}C age calibration program, Radiocarbon, 35, 215-230, 1993.

Ślubowska-Woldengen, M., Rasmussen, T.L., Koç, N., Klitgaard-Kristensen, D., Nilsen, F., Solheim, A.: Advection of Atlantic Water to the western and northern Svalbard shelf since 17,500 cal yr BP. Quat. Sci. Rev., 26 463-478, https://doi.org/10.1016/j.quascirev.2006.09.009, 2007.

Telesiński, M.M., Przytarska, J.E., Sternal, B., Forwick, M., Szczuciński, W., Łącka, M., Zajączkowski, M.: Palaeoceanographic evolution of the SW Svalbard shelf over the last 14 000 years, Boreas, 47, 410-422, https://doi.org/10.1111/bor.12282, 2018.

Thomsen, P.F., Willerslev, E.: Environmental DNA – An emerging tool in conservation for monitoring past and present biodiversity, Biol. Conserv., 183, 4-18, https://doi.org/10.1016/j.biocon.2014.11.019, 2015.

Werner, K., Spielhagen, R.F., Bauch, D., Hass, H., Kandiano, E.S., Zamelczyk, K.: Atlantic Water advection to the eastern Fram Strait – multiproxy evidence for late Holocene variability. Palaeogeogr. Palaeoclimatol. Palaeoecol., 308, 264-276, https://doi.org/10.1016/j.palaeo.2011.05.030, 2011.

Winkelmann, D., Knies, J.: Recent distribution and accumulation of organic carbon on the continental margin west off Spitsbergen. Geochem. Geophys. Geosyst., 6, Q09012, https://doi.org/10.1029/2005GC000916, 2005.

Wollenburg, J.E., Kuhnt, W.: The response of benthic foraminifers to carbon flux and primary production in the Arctic Ocean, Mar. Micropaleontol., 40, 189-231, https://doi.org/10.1016/S0377-8398(00)00039-6, 2000.

Figures captions

Figure 1: Study area and the location of the studied core ST_1.5 and the other cores discussed in this paper.

Figure 2: Temperature and salinity profile from the sampling station. Temperature is marked with a dashed line, and salinity is marked with a black line. Abbreviations: AW – Atlantic Water, TAW – Transformed Atlantic Water, BSW – Brine-enriched Shelf Water.

Figure 3: Age–depth model of the studied core.

Figure 4: Sedimentological and micropaleontological data plotted versus age. The sediment accumulation rate (SAR), mean grain size of the 0-63-μm fraction, ice-rafted debris (IRD) flux and number of grains per gram of sediment, oxygen ($\delta^{18}O$) and carbon ($\delta^{13}C$) stable isotopes in foraminiferal tests, the percentage of calcareous foraminifera individuals and the flux and abundance of foraminifera are presented.

Figure 5: The abundance (expressed as the number of individuals per gram of dry sediment) and the percentage of the dominant testate foraminifera.

Figure 6: The dominant components of the monothalamous assemblages. The abundance is expressed as the percentage of the monothalamous sequences and the most abundantly sequenced taxa are presented. The trend is indicated with the dashed line.

Figure 7: The percentage share of certain clades in the allogromiid sequences.

Figure 8: The percentage of sequences of dominant diatom taxa vs. time. The trend is indicated with the dashed line.

Tables captions

Table 1: Raw and calibrated AMS^{14}C dates used in the age model.

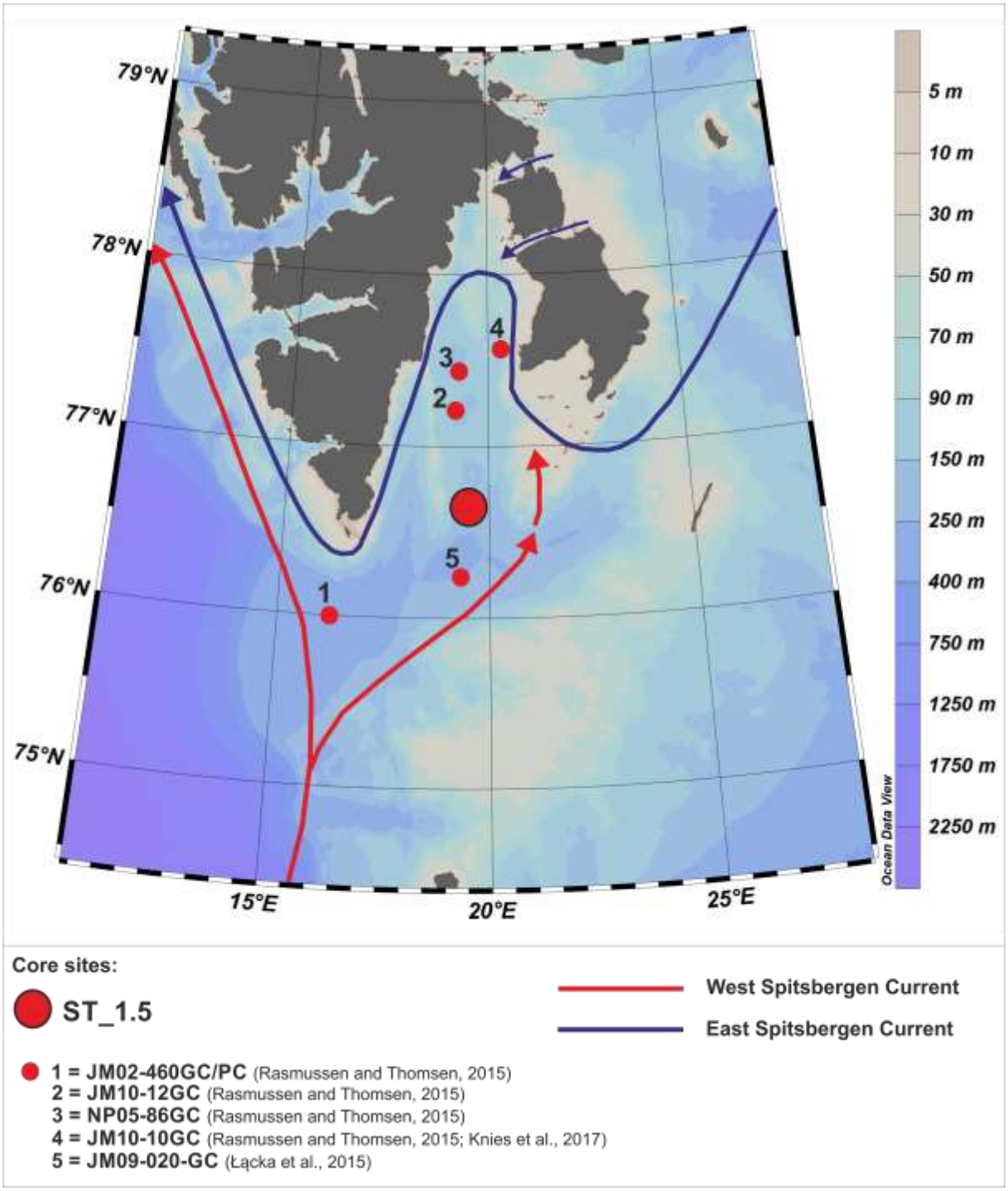

Figure 1: Study area and the location of the studied core ST_1.5 and the other cores discussed in this paper.

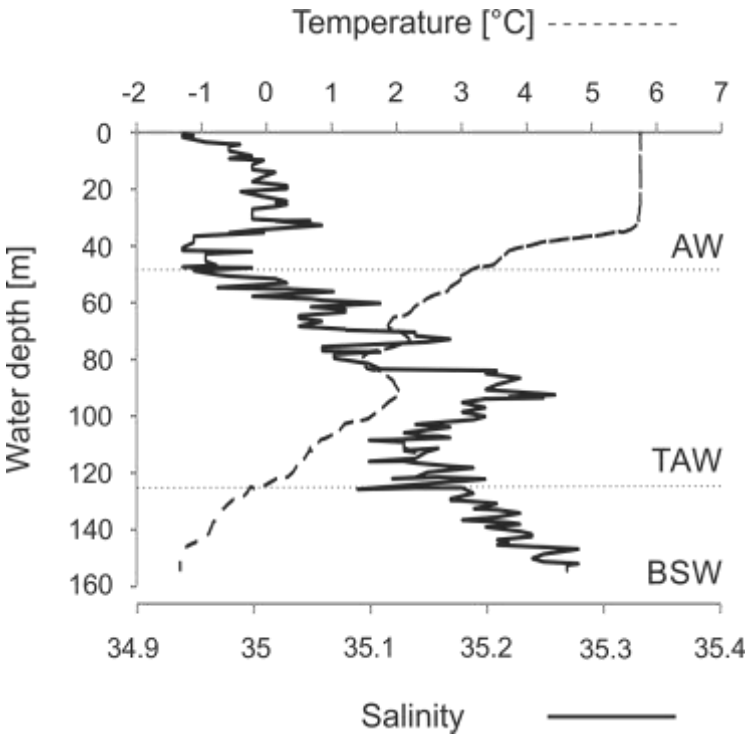

Figure 2: Temperature and salinity profile from the sampling station. Temperature is marked with a dashed line, and salinity is marked with a black line. Abbreviations: AW – Atlantic Water, TAW – Transformed Atlantic Water, BSW – Brine-enriched Shelf Water.

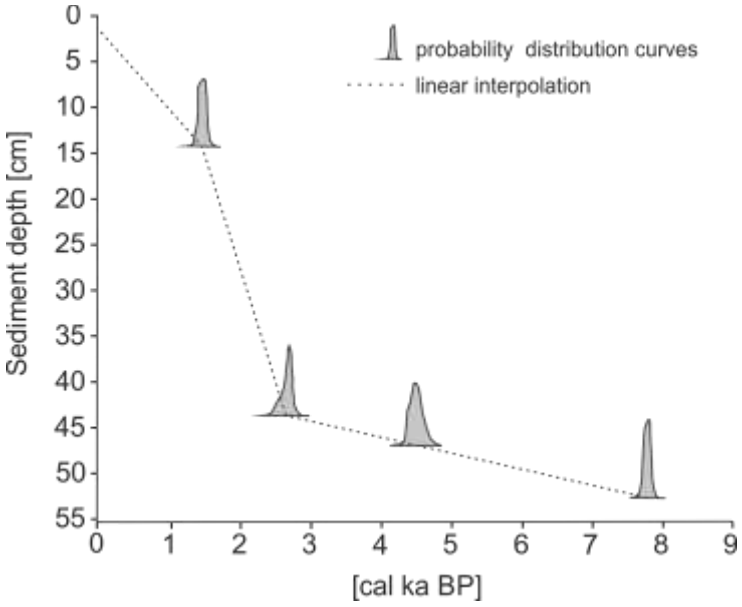

Figure 3: Age-depth model of the studied core.

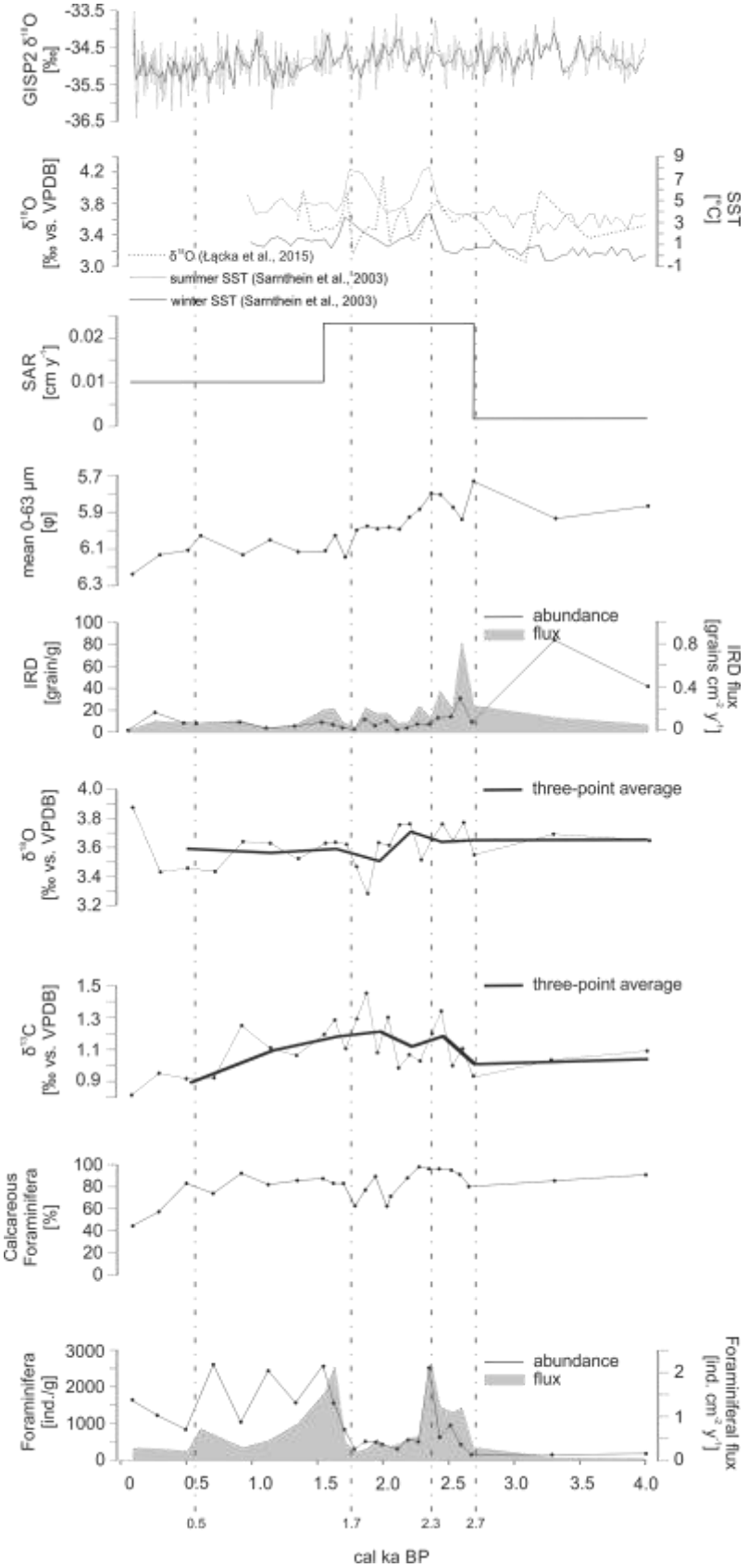

Figure 4: Sedimentological and micropaleontological data plotted versus age. The sediment accumulation rate (SAR), mean grain size of the 0-63-µm fraction, ice-rafted debris (IRD) flux and number of grains per gram of sediment, oxygen ($\delta^{18}O$) and carbon ($\delta^{13}C$) stable isotopes in foraminiferal tests, the percentage of calcareous foraminifera individuals and the flux and abundance of foraminifera are presented.

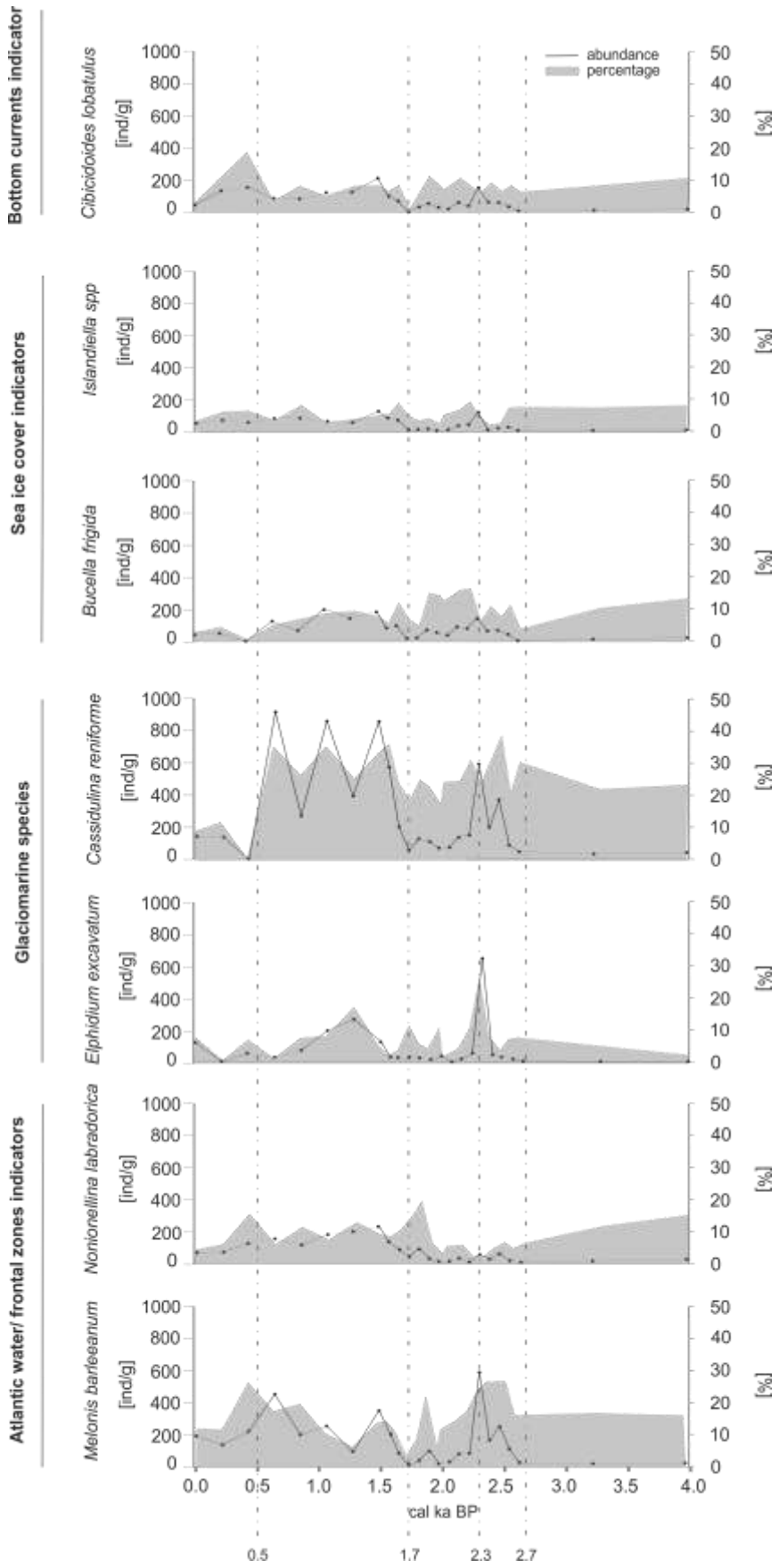

Figure 5: The abundance (expressed as the number of individuals per gram of dry sediment) and the percentage of the dominant testate foraminifera.

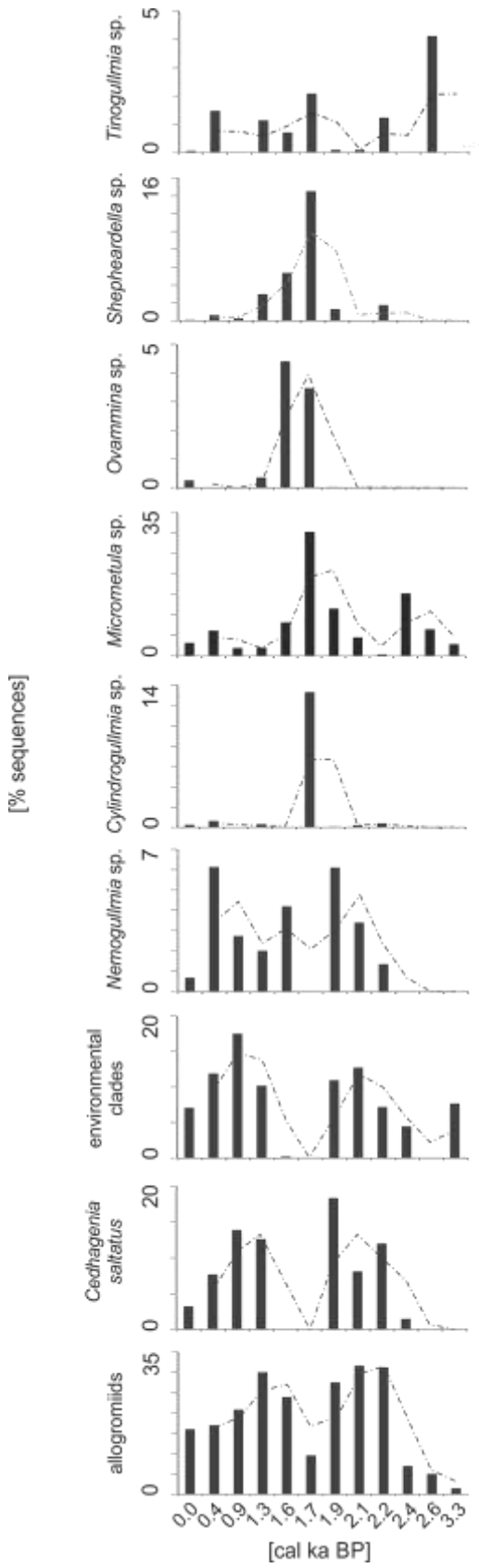

Figure 6: The dominant components of the monothalamous assemblages. The abundance is expressed as the percentage of the monothalamous sequences and the most abundantly sequenced taxa are presented. The trend is indicated with the dashed line.

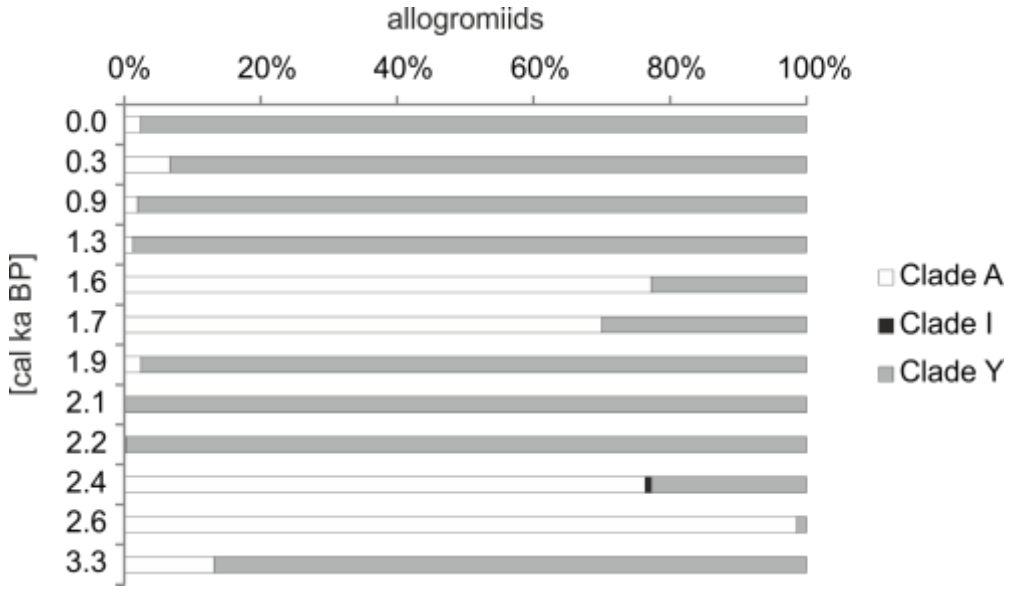

Figure 7: The percentage share of certain clades in the allogromiid sequences.

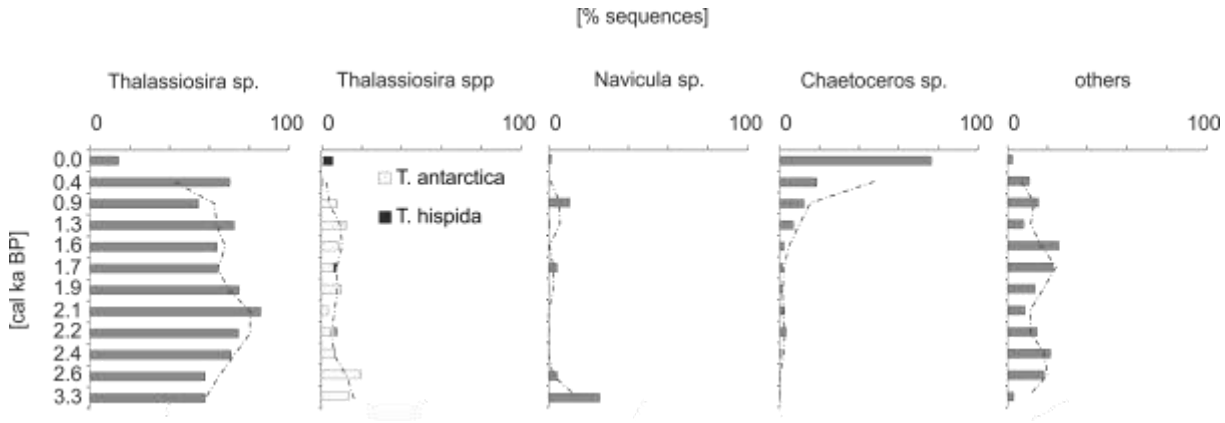

Figure 8: The percentage of sequences of dominant diatom taxa vs. time. The trend is indicated with the dashed line.

1 **Table 1:** Raw and calibrated AMS ^{14}C dates used in the age model.

Sediment depth [cm]	Material	Raw AMS ^{14}C	Calibrated years BP ± 2σ	Cal. a BP used in age model
2.5	*Nuculana pernula*	107.38 ± 0.33 pMC	-	-
5.5	*Yoldiella lenticula*	290 ± 30 BP	-	-
14.5	*Turitella erosa*	2020 ± 30 BP	1356-1555	1500
43.5	*Yoldiella solituda*	3010 ± 50 BP	2484-2787	2700
46.5	*Nonionellina labradorica*	4490± 40 BP	4400-4701	4500
52.5	*Yoldiella lenticula*	7545 ± 35 BP	7803-7989	7890

2